RESEARCH ARTICLE OPEN ACCESS

A Consecutive Genome Engineering Method Reveals a New Phenotype and Regulation of Glucose and Glycerol Utilization in *Clostridium Pasteurianum*

Tom Nguyen[1] [iD] | Luca W. G. Meleski[1] | Minu P. Belavatta[1] | Sivasubramanian Gurumoorthi[1] | Chijian Zhang[1,2] | Anna-Lena Heins[1] | An-Ping Zeng[1,3] [iD]

[1]Institute of Bioprocess and Biosystems Engineering, Hamburg University of Technology, Hamburg, Germany | [2]Hua An Tang Biotech Group Co., Ltd, Guangzhou, China | [3]Center of Synthetic Biology and Integrated Bioengineering, School of Engineering, Westlake University, Hangzhou, China

Correspondence: An-Ping Zeng (aze@tuhh.de; zenganping@westlake.edu.cn)

ABSTRACT

Clostridium pasteurianum is a microorganism for production of 1,3-propanediol (1,3-PDO) and butanol, but suffers from lacking genetic tools for metabolic engineering to improve product titers. Furthermore, previous studies of *C. pasteurianum* have mainly focused on single genomic modification. The aim of this work is the development and application of a method for modification of multiple gene targets in the genome of *C. pasteurianum*. To this end, a new approach for consecutive genome engineering is presented for the first time using a method based on endogenous CRISPR-Cas machineries. A total of three genome modifications were consecutively introduced in the same mutant and the effect of combined changes on the genome was observed by 39% decreased specific glycerol consumption rate and 29% increased 1,3-PDO yield in mixed substrate fermentations at laboratory scale in comparison to the wildtype strain. Additionally, examination of the phenotype of the generated mutant strain led to discovery of 2,3-butanediol (2,3-BDO) production of up to 0.48 g L^{-1}, and this metabolite was not reported to be produced by *C. pasteurianum* before. The developed procedure expands the genetic toolkit for *C. pasteurianum* and provides researchers an additional method which contributes to improved genetic accessibility of this strain.

1 | Introduction

The anaerobic and gram-positive microorganism *Clostridium pasteurianum* R525 (R525) is known for production of its main metabolite butanol in fermentations with glycerol as carbon source and for its improved transformation efficiency in comparison to *C. pasteurianum* DSM 525 from which it originates [1–3]. Furthermore, unique advantages of the newly isolated strain *C. pasteurianum* C8 (C8) enabled the development of an industrial 1,3-PDO production process with high productivity of up to 5.33 g L^{-1} h^{-1} with pure glycerol as substrate [4–6]. The main difference is that R525 carries two additional butanol dehydrogenase genes (*adh2*, *bdhA2*) and does not carry a second 1,3-PDO dehydrogenase gene (*dhaTC8*) [5] in comparison to C8. *C. pasteurianum* is also able to metabolize glycerol and glucose together in mixed substrate fermentations [1], but deletion of multiple gene targets of competing pathways would be required to enable the formation of 1,3-PDO solely from the renewable

Summary

• Previous synthetic biology works with *Clostridium pasteurianum* mainly created mutants with single genomic modification, but deletion of multiple genes of competing pathways is necessary for stable introduction of novel pathways.

• For this purpose, a new procedure is provided to enable consecutive genome modifications such as gene deletions or replacements.

• It is the first time that the endogenous CRISPR-Cas method was applied to delete several genes in a single mutant of *C. pasteurianum*.

• Curing of large genome editing plasmids, which contain a CRISPR array, was not possible before. However, this was successfully addressed with the presented method which can be applied without the need for a specific host strain.

• The developed method gives the opportunity to simply modify the genome of *C. pasteurianum* in a customized manner for desired applications.

resource glucose. This was already achieved by development of recombinant *E. coli*, which can reach a 1,3-PDO production rate of 3.50 g L^{-1} h^{-1} in fed-batch fermentations with glucose [7, 8]. However, research studies based on these strains were prevented due to broad patenting. As a result, other microorganisms such as *Klebsiella pneumoniae* [9] or *Corynebacterium glutamicum* [10] were engineered to produce 1,3-PDO from glucose.

In the case with *C. pasteurianum*, studies have shown that previously unknown pathways and phenotypes were uncovered through metabolic engineering. For instance, the glycine synthase system from *Gottschalka acidurici* was introduced into R525 [3] for conversion of the C1 components formate and CO_2 [11]. This triggered formation of 2-oxobutryate and in another study, a previously unknown formation of 1,2-propanediol (1,2-PDO) was identified while deletion of 1,3-PDO dehydrogenase increased 1,2-PDO production by 5-fold [12]. Previous metabolic engineering studies of *C. pasteurianum* elaborated different methods, for example, utilization of endogenous CRISPR-Cas machineries [13], CRISPR-Cas9-nickase [3] and Allele-Coupled Exchange (ACE) [14, 15], and reported genome modifications include deletion of genes such as *cpaAIR*, *dhaT*, *spo0A*, *spoIIE*, *hydA*, *rex*, or *dhaB* (Table S1). However, the applied methods mainly focused on single genomic modification. Only one previous work carried out successive modifications with the ACE method which was not reported for the endogenous CRISPR-Cas method yet.

While simultaneous targeting of multiple genes is limited with utilization of Cas9 because multiple expression constructs are necessary, a single CRISPR array with multiple target sequences (spacers) can be used for editing of several genes with Cas12a [16]. Multiplex genome editing with CRISPR-Cas systems was demonstrated in the genus of *Streptomyces* [17, 18], *E. coli* [19], and *Streptococcus* [20]. Moreover, a concept of a two-plasmid system was applied before in *C. beijerinckii* and *C. acetobutylicum* to separately introduce the *cas9* gene and guide RNA (gRNA) with editing templates [21, 22]. It would be beneficial to transfer these genome editing tools to *C. pasteurianum*, but expression of *cas9* can be toxic to *C. pasteurianum* cells and transformation efficiency was observed to decrease with increasing plasmid size [3, 13, 23].

The objective of the present study is to initiate a first step toward improved 1,3-PDO synthesis from glucose in *C. pasteurianum* R525 by genetic engineering, which is impossible so far in naturally higher producer such as the strain C8. Therefore, the basis for genetic engineering was to utilize the differences between both strains. Furthermore, a glycerol synthesis pathway from *Saccharomyces cerevisiae* with the two enzymes glycerol-3-phosphate dehydrogenase (*GPD1*) and glycerol-1-phosphatase (*GPP2*) needs to be introduced [24, 25]. To enable multiple consecutive genetic modifications in *C. pasteurianum*, this study developed a consecutive genome engineering (CGE) method, which is based on the endogenous CRISPR-Cas method. The focus was also to develop a simpler method compared to the ACE method in order to create an alternative method for the scientific community.

Overall, application of the developed CGE method was applied by introducing a total of three genome modifications into a single *C. pasteurianum* mutant. Batch fermentations were carried out for characterization of the generated mutants in comparison to the wildtype strain to determine how the metabolic engineering influenced the production phenotype.

2 | Materials and Methods

2.1 | Bacterial Strains and Plasmid Construction

Strains, plasmids and synthetic DNA used in this study are summarized in Table 1. *E. coli* 10-beta (New England Biolabs, USA) and *C. pasteurianum* R525 [3] strains were stored at 80°C in ROTI Store cryo vials (Carl Roth GmbH + Co. KG, Germany) or cryogenic vials (Carl Roth GmbH + Co. KG, Germany) with 1.8 mL grown cultures containing 20% (v v^{-1}) glycerol, respectively. The whole genome of the strain *C. pasteurianum* DSM 525 was sequenced in 2015 and was reported to have a total length of 4,351,673 bp [26] and this complete genome sequence was used in this study. Components for constructed plasmids in this work (Supporting Information 2) were amplified by polymerase chain reaction (PCR) using CloneAmp HiFi PCR Premix (Takara Bio Inc., Japan) with primers (Table S3) purchased from Integrated DNA Technologies Inc. (USA). PCR samples were extracted with NucleoSpin Gel and PCR Clean-up (Macherey-Nagel GmbH & Co. KG, Germany). Extracted plasmid components were fused with In-Fusion cloning (Takara Bio Inc., Japan). Constructed plasmids were transformed into *E. coli* 10-beta for plasmid propagation and subsequently into *E. coli* 10-beta+pFnuDIIMKn [27] for methylation (Supporting Information 3). Correct plasmid sequence was confirmed with Sanger sequencing (Microsynth Seqlab GmbH, Germany).

2.2 | Consecutive Genome Engineering (CGE)

The CGE method utilizes the endogenous CRISPR-Cas method [13] and the main principle is to facilitate plasmid curing

Table 1 | Strains, plasmids, and synthetic DNA used in this work.

Strain/plasmid	Abbreviation	Characteristics	Reference
E. coli			
10-beta		Dam + methylation	New England Biolabs (USA)
10-beta + pFnuDIIMKn		Dam + and *CpaAI* methylation	[11, 27]
C. pasteurianum			
R525	R525	DSM No.: 117789, improved transformation efficiency, originates from *C. pasteurianum* DSM 525	[3], DSMZ
R525+pAR	AR-I	$adh2^{dhaTC8+}$	This study
R525+pAR+pBD	BD-II	$adh2^{dhaTC8+}$, $bdhA2^-$	This study
R525+pAR+pBD+pDR	DR-III	$adh2^{dhaTC8+}$, $bdhA2^-$, $dhaD1\_dhaK^{GPD1\_GPP2+}$	This study
R525+pDR	DR-I	$dhaD1\_dhaK^{GPD1\_GPP2+}$	This study
Plasmids			
pMTL85141		pIM13, *catP*, ColE1	[28]
pMTL82254		pBP1, *ermB*, ColE1	[28]
pMTL84422		pCD6, *tetA*, p15a	[28]
pMTL-GCSY1		pIM13, *catP*, ColE1, glycine synthase from *Gottschalkia acidurici*	[11]
pMTL007-PC		pCB102, *catP*, pyruvate carboxylase from *C. pasteurianum*	[29]
p_adh2-rpl	pAR	pCB102, *catP*, ColE1, repair template for *adh2* replacement with *dhaTC8*	This study
p_bdhA2-del	pBD	pIM13, *ermB*, ColE1, repair template for *bdhA2* deletion	This study
p_dhaD1-rpl	pDR	pCB102, *catP*, ColE1 repair template for *dhaD1* and *dhaK* replacement with *GPD1* and *GPP2*	This study
Synthetic DNA			
Pthl_1200-9-9_gpd1		Contains the gene *GPD1* and promoter	Thermo Fisher Scientific Inc. (USA)
Pfdx_gpp2_fdx_term		Contains the gene *GPP2*, promoter and terminator	
dhaD1_CRISPR_array		CRISPR array for targeting *dhaD1*	
adh2_CRISPR_array		CRISPR array for targeting *adh2*	
bdhA2_CRISPR_array		CRISPR array for targeting *bdhA2*	

Abbreviations: $bdhA2^-$: *bdhA2* deleted; *catP*, *ermB*, *tetA*: antibiotic resistance markers against chloramphenicol/thiamphenicol, erythromycin, and tetracycline, respectively. *dhaTC8+*: replaced by *dhaTC8*; ColE1 and p15a: gram-negative replicons; *dhaD1_dhaK*: *dhaD1* and *dhaK*; *GPD1_GPP2+*: replaced by *GPD1* and *GPP2*.; pIM13, pBP1, pCD6 and pCB102: gram-positive replicons.

as a crucial requirement for successive modifications. Based on gene differences between R525 [3] and the efficient 1,3-PDO producing strain C8 [5], following modifications were carried out (Figure 1). The first modification replaced gene *adh2* (CPAST_c33950) with *dhaTC8*, second modification deleted *bdhA2* (CPAST_c15980), third modification replaced *dhaD1* and *dhaK* (CPAST_c12160, CPAST_c12150) with *GPD1* and *GPP2*. *GPD1* catalyzes the conversion of the glycolysis intermediate dihydroxyacetone phosphate (DHAP) to glycerol-3-phosphate, which is then converted to glycerol by *GPP2* [24, 25]. 1,3-PDO

can then be produced by the native pathway from which the reaction steps are catalyzed by the glycerol dehydratase and 1,3-PDO dehydrogenase (Figure 1). These genome modifications were introduced successively with plasmids p_adh2-rpl (pAR), p_bdhA2-del (pBD), and p_dhaD1-rpl (pDR) as described below. Homologous recombination occurs with the help of DNA sequences which are 1000 bp upstream (H1) and 1000 bp downstream (H2) of the gene to be deleted or replaced. These sequences are cloned on the genome editing plasmids to create the editing template [13].
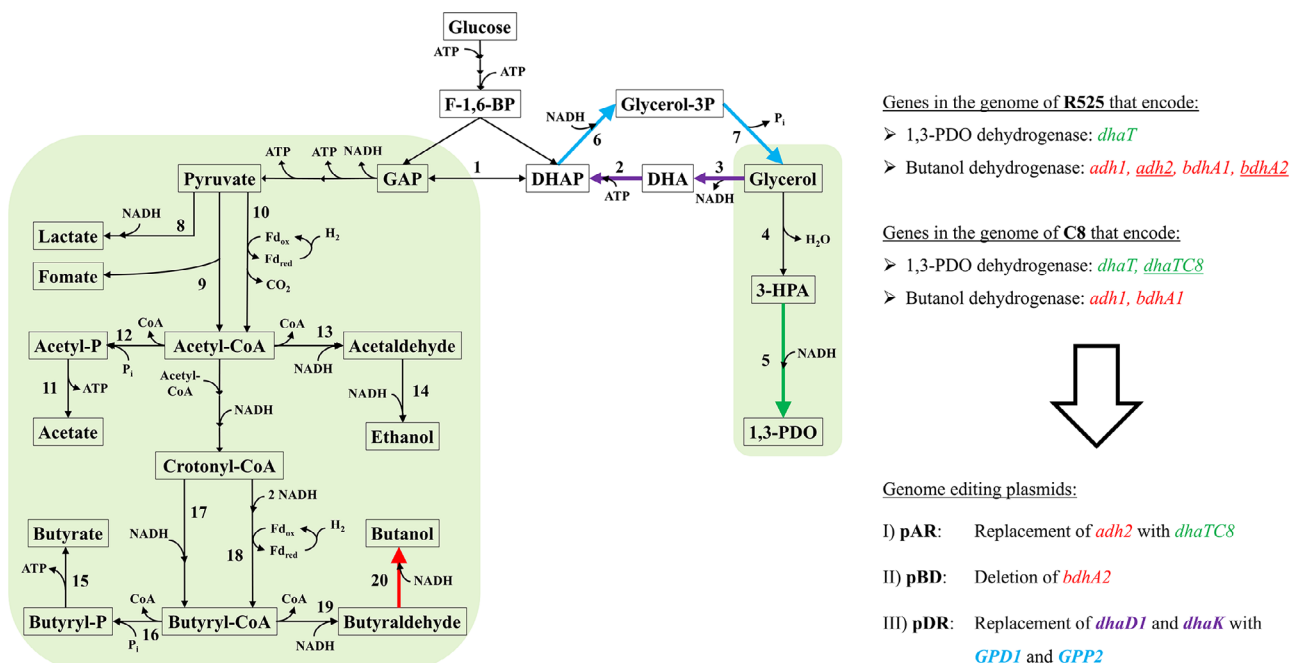
Figure 1 | Metabolism of *C. pasteurianum* and genome editing targets. Genes encoding enzymes are numbered as follows: 1, triose-phosphate isomerase (*tpiA*); 2, dihydroxyacetone kinase (*dhaK*); 3, glycerol dehydrogenase (*dhaD1*, *dhaD2*); 4, glycerol dehydratase; 5, 1,3-PDO dehydrogenase (*dhaT*); 6, glycerol-3-phosphate dehydrogenase (*GPD1*); 7, glycerol-1-phosphatase (*GPP2*); 8, lactate dehydrogenase; 9, pyruvate formate-lyase; 10, pyruvate:ferredoxin oxidoreductase; 11, acetate kinase; 12, phosphate acetyltransferase; 13, acetaldehyde dehydrogenase; 14, ethanol dehydrogenase; 15, butyrate kinase; 16, phosphate butyryltransferase; 17, butyryl-CoA dehydrogenase; 18, ferredoxin-dependent butyryl-CoA dehydrogenase/electron transferring flavoprotein complex; 19, butyraldehyde dehydrogenase; 20, butanol dehydrogenase (*adh1*, *adh2*, *bdhA1*, and *bdhA2*). 3-HPA, 3-hydroxypropionic aldehyde; 3P, 3-phosphate; F-1,6-BP, fructose 1,6-bisphosphate; *dhaTC8*, 1,3-PDO dehydrogenase from *C. pasteurianum* C8. The figure was adapted from [15, 30].

2.2.1 | Wildtype R525 Was Transformed With pAR (Figure 2A)

A novel plasmid design was implemented to enable plasmid curing: each plasmid was designed to carry a part of the sequence of the next gene target which will be deleted in the subsequent genome engineering step. Therefore, plasmid pAR carries part of gene *bdhA2* and plasmid pBD carries part of gene *dhaD1*. First, R525 was transformed with plasmid pAR and resulting mutant R525+pAR (AR-I) was isolated by selection on agar plates with 10 μg mL^{-1} thiamphenicol (Tm10). Methylated plasmids were transformed into *C. pasteurianum* by the electrotransformation protocol [27], which was adapted by Hong et al. [11].

2.2.2 | Transformation of pBD Into Mutant AR-I (Figure 2B)

Alternating antibiotic markers were necessary for the selection procedure and several markers were tested besides the previously used *catP* marker (Supporting Information 4). Consequently, a new approach was applied and verified where antibiotic markers *tetA* (plasmid propagation and methylation) and *ermB* (*C. pasteurianum* transformation) were combined on plasmid pBD. In the second step, mutant AR-I was transformed with plasmid pBD, and selection was carried out on agar plates with 300 μg mL^{-1} erythromycin (Em300).

2.2.3 | Simultaneous Targeting of pAR and Genome (Figure 2C)

At the same time, transcription of precursor CRISPR-RNA (crRNA) from the CRISPR array of plasmid pBD and subsequent processing by Cas6 endonuclease to mature crRNA occurs [13]. This leads to complementary annealing of mature crRNA to the recognition sequence, which is present on gene *bdhA2* within the genome and on plasmid pAR. Afterwards, the Cas3 endonuclease introduces a DNA nick [13, 32, 33].

2.2.4 | Creation of Mutant BD-II (Figure 2D)

This ultimately results in survival of cells only with deleted gene *bdhA2* and simultaneously cured plasmid pAR. Before introducing plasmid pDR, the resulting mutant AR-I+pBD (BD-II) was re-plated on fresh agar plates with Em300 for three times to ensure complete curing of the first plasmid pAR. After the re-plating procedure, the mutant BD-II was plated on agar plates with Tm10 to check if mutant BD-II can still grow on agar plates with thiamphenicol.

2.2.5 | Repeating Steps B-C With Plasmid pDR (Figure 2E)

Final mutant BD-II+pDR (DR-III) was isolated by selection with Tm10, same antibiotic as in the first step. Mutant DR-III was
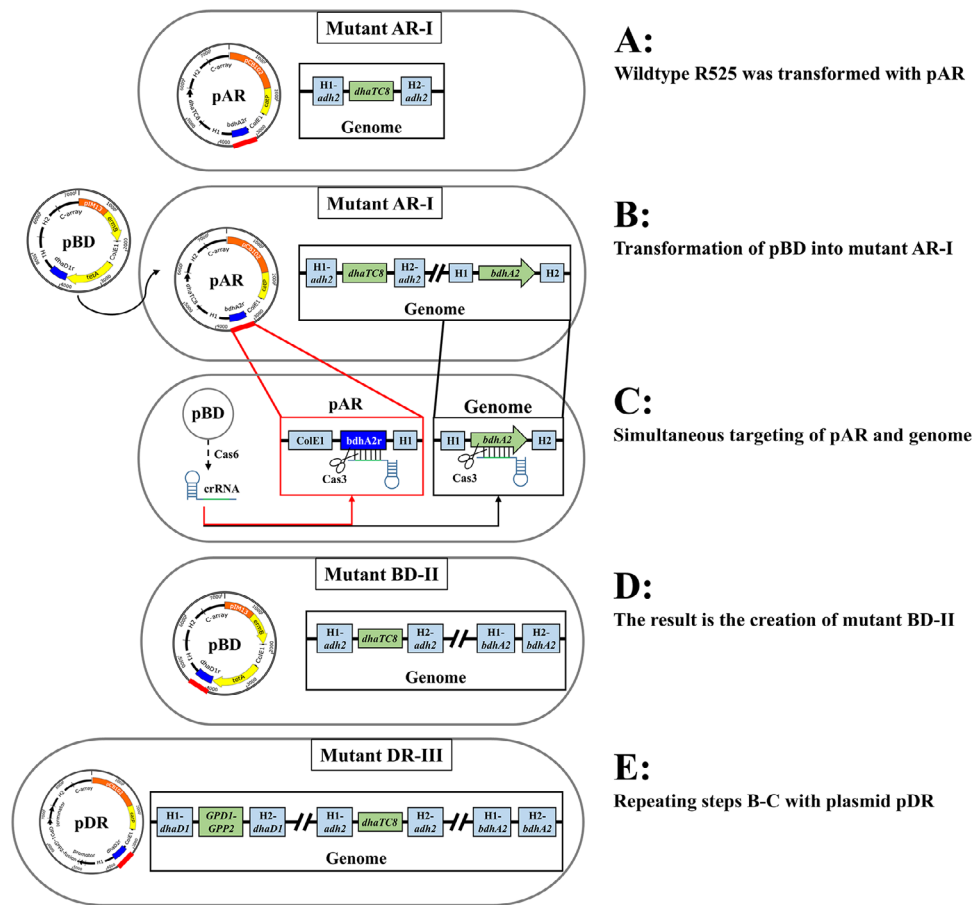
Figure 2 | Schematic overview of steps for the consecutive genome engineering method. (A) Mutant R525+pAR (AR-I) was isolated by selection with 10 µg mL^{-1} thiamphenicol (Tm10) after electrotransformation of plasmid pAR into R525. (B) Electrotransformation of plasmid pBD into mutant AR-I and selection with 300 µg mL^{-1} erythromycin (Em300). (C) Simultaneous targeting of gene *bdhA2* on the genome and on plasmid pAR by transcription of crRNA from plasmid pBD. (D) Plasmid pAR was cured from the cells and *bdhA2* was deleted, resulting in mutant BD-II. (E) Steps B-C are repeated with plasmid pDR and selection with Tm10, resulting in mutant DR-III with three genome modifications. The orange and yellow colored plasmid components are alternating for each genome modification step: orange: gram-positive replicon (pCB102 or pIM13), yellow: antibiotic markers (*catP* or *ermB* and *tetA*), blue: target region of the next plasmid for genome engineering. C-array, CRISPR array; ColE1, gram-negative replicon; H1, H2, homologous regions upstream and downstream of the targeted gene; *dhaTC8*, 1,3-PDO dehydrogenase from *C. pasteurianum* C8; bdhA2r, dhaD1r, dhaD2r, part of the genes encoding *bdhA2*, *dhaD1* or *dhaD2*; promoter/terminator, Csp fdx promoter and terminator from pMTL007CE2 [31].

again re-plated on fresh agar plates with Tm10 for three times for complete removal of the second plasmid pBD which enables further genome engineering steps. In order to examine the effect of two deleted butanol dehydrogenase genes on 1,3-PDO production from glucose with mutant DR-III, an additional mutant was created by transformation of plasmid pDR into wildtype R525, resulting in mutant R525+pDR (DR-I). All procedures were carried out within an anaerobic chamber (Coy Laboratory Products Inc., USA).

2.3 | Characterization of *C. pasteurianum* in a Bioreactor

2.3.1 | Pre-Cultures

A two-step pre-culture procedure was performed. A first pre-culture with 50 mL of 2xYTG medium (5 g L^{-1} glucose, 0.2 mg L^{-1} resazurin, 0.5 g L^{-1} cysteine*HCl*H$_2$O, 31 g L^{-1} 2xYT medium (Carl Roth GmbH + Co. KG, Germany) consisting of 16 g L^{-1} tryptone, 10 g L^{-1} yeast extract, and 5 g L^{-1} NaCl, pH 6.5) was inoculated with 1.8 mL cryo-stock culture of either R525 or DR-III. This first pre-culture was incubated anaerobically in a serum bottle for 16 h at 35°C without agitation. For the second pre-culture, 5 mL of the first pre-culture were inoculated into 100 mL of modified synthetic (MS) medium (10 mg L^{-1} FeSO$_4$*7H$_2$O, 3 g L^{-1} (NH$_4$)$_2$SO$_4$, 0.75 g L^{-1} KCL, 2.45 g L^{-1} NaH$_2$PO$_4$*H$_2$O, 4.58 g L^{-1} Na$_2$HPO$_4$, 0.28 g L^{-1} Na$_2$SO$_4$, 0.42 g L^{-1} C$_6$H$_8$O$_7$*H$_2$O, 0.26 g L^{-1} MgCl$_2$*6H$_2$O, 0.009 g L^{-1} CaCl$_2$*2H$_2$O, 1 g L^{-1} yeast extract, 2 g L^{-1} CaCO$_3$, 0.2 mg L^{-1} resazurin, 2 mL trace element solution [34]). Resazurin was supplemented to ensure that anaerobic conditions were maintained. The second pre-culture was incubated anaerobically in a serum bottle for 24 h at 35°C without agitation.

2.3.2 | Bioreactor Cultures

Fermentations with wildtype R525 and mutant DR-III were carried out with supplementation of 80 g L^{-1} glucose as the

sole carbon source or with 80 g L^{-1} glucose and 20 g L^{-1} glycerol. The fermentations were carried out in a 4-fold parallel cultivation system with 1.5 L DASGIP bioreactors without baffles (Eppendorf SE, Germany) with a working volume of 1 L. A two-point calibration, using pH values of 4 and 7, was carried out for pH probes. After autoclaving the bioreactors with 1 L MS medium (100 mg L^{-1} FeSO$_4$*7H$_2$O instead of 10 mg L^{-1}) for 20 min at 121°C, the temperature, stirrer (2× Rushton impeller, overhead drive) and nitrogen gassing (L-Sparger) were set to 35°C, 400 rpm and 6 L h^{-1}, respectively. The pH was controlled at 6.5 through titration with 5 M KOH during the batch fermentations. Fifty milliliters of the second pre-culture with an OD$_{600}$ value over 4.0 was inoculated into the bioreactor and gassing was stopped. Sample volumes of 2 mL were taken regularly to cover all growth phases throughout the batch fermentations for analysis of biomass and metabolite concentrations. The first sample was taken directly after inoculation with the second pre-culture.

2.4 | Analytical Methods

2.4.1 | Determination of Biomass Concentration

To examine the samples, the optical density OD_{600} of the cell suspension was determined by photometric turbidity measurement using a UV/Vis spectrophotometer (VWR International GmbH, USA) at a wavelength of 600 nm. Samples for OD_{600} measurement were diluted at least with a factor of 1:4 with 0.1% HCL to remove the undissolved calcium carbonate. The dilution rate was increased when OD_{600} values reached higher values than 0.6 and less sample volume was used for the OD_{600} measurement accordingly. The concentration of bio dry mass (BDM) c_X in g L^{-1} can be calculated according to Groeger et al. by multiplying OD_{600} with a correlation factor of 0.336 [30].

2.4.2 | Determination of Metabolite Concentrations

The remaining sample was centrifuged for 4 min at 4°C and 13,000 rpm in a benchtop centrifuge (Thermo Fisher Scientific Inc., USA) and the supernatant was sterile filtered using a filter with a pore size of 0.22 µm (Carl Roth GmbH + Co. KG, Germany). All filtered samples were diluted in a ratio of 1:2 and stored at 20°C as preparation for high-performance liquid chromatography (HPLC) measurement. The concentrations of glucose, glycerol, ethanol, butanol, 1,3-PDO, lactate, formate, acetate, and butyrate were determined via HPLC with UV and RI detectors (Knauer, Germany) [1]. The mobile phase was 0.1% trifluoroacetic acid (TFA), a flow rate of 0.6 mL min^{-1} was set and the column temperature was 60°C. It was necessary to determine whether 1,3-PDO detected by HPLC corresponds to 1,3-PDO or another product such as 1,2-propanediol (1,2-PDO). Hence, samples from fermentations with only glucose were analyzed via gas chromatography coupled to mass spectrometry (GC-MS). The measurement was carried out using a 7890B GC System with a 5977A mass selective detector (MSD) (Agilent Technologies Inc., USA), an Agilent HP5-ms capillary column (30 m*0.25 mm*0.25 µm), and helium as carrier gas (1 mL min^{-1}). The temperature of the oven program was set to 100°C for 2 min, increased by 10°C min^{-1} to 270°C and 270°C for 7 min.

2.5 | Fermentation Data Analysis

The following calculations were performed using Excel (Microsoft Corporation, USA). The overall substrate-specific yield $Y_{P/S}$ in g g^{-1} can be calculated according to Equation (1) with measured concentrations c_i in g L^{-1}.

$$Y_{P/S} = \frac{c_p(t) - c_p(t_0)}{c_s(t_0) - c_s(t)} \quad (1)$$

With $c_i(t)$, $c_i(t_0)$: concentration of a product p or substrate s at time point t or $t = 0$. The maximum specific growth rate μ in h^{-1} was calculated using Equation (2) by determining the slope from linearized values of the natural logarithm of biomass concentrations in the exponential growth phase. With $c_{x,2}$, $c_{x,1}$: biomass concentrations at time points t_2 and t_1, respectively.

$$\mu_{max} = \frac{\ln c_{x,2} - \ln c_{x,1}}{t_2 - t_1} \quad (2)$$

The specific formation or consumption rates q_i in g g$_{biomass}$$^{-1}$ h^{-1} were calculated using Equation (3) with formed product p or consumed substrate s in the interval between two time points.

$$q_i = \frac{dc_i}{c_x \cdot dt} \quad (3)$$

Theoretical molar concentration of carbon dioxide c_{CO_2} in mmol L^{-1} was calculated with measured concentrations and respective molar masses M_i in following Equation (4), according to the metabolism of *C. pasteurianum* (Figure 1) [35].

$$c_{CO_2} = \frac{c_{ethanol}}{M_{ethanol}} + \frac{c_{acetate}}{M_{acetate}} + 2 \cdot \left(\frac{c_{butanol}}{M_{butanol}} + \frac{c_{butyrate}}{M_{butyrate}} \right) - \frac{c_{formate}}{M_{formate}} \quad (4)$$

Carbon molar concentrations $c_{C,i}$ in mmol$_C$ L^{-1} were calculated using the molar mass and by multiplying measured metabolite concentrations by the respective number of carbon atoms. The carbon distribution $C_{distribution,p}$ of a product p in % can be determined by forming the ratio between the formed product $\Delta c_{C,p}$ and the sum of all products as shown in Equation (5).

$$C_{distribution,p} = \frac{\Delta c_{C,p}}{\sum \Delta c_{C,p}} \quad (5)$$

3 | Results and Discussion

3.1 | Introduced Consecutive Genome Modifications

All three genome modifications introduced into *C. pasteurianum* R525 were verified by PCR amplification (Supporting Information 5) of the respective target regions. Sanger sequencing confirmed correct gene deletions (mutant BD-II) and replacements (mutants AR-I and DR-III). Hence, consecutive genome modifications were successfully enabled with the developed CGE method in this work. Two plasmids (pAR, pBD) had to be consecutively cured from the mutant strain and it needs to be considered that there could be general difficulties. Different plasmid sizes or

plasmid components, for example, stronger replication origin, could influence the efficiency of plasmid curing and if the recognition sequence of the targeted gene is already present on essential parts of the plasmid, re-design might not be possible in every case. Apart from that, it is possible that there are genes that cannot be deleted due to absent or unrecognized target sequences. It's crucial to consider these points for future applications of the developed CGE method.

For the designed plasmids of this study, utilized spacer sequences were chosen to be only homologous to the targeted gene and not to other components of the respective plasmid. No growth was observed for mutant BD-II and DR-III on agar plates supplemented with thiamphenicol or erythromycin, respectively, after the replating procedure (data not shown). The results indicate that plasmid pBD targeted and degraded the first plasmid pAR successfully and introduction of plasmid pDR removed the second plasmid pBD.

Multiple genome modifications in a single *C. pasteurianum* mutant were previously only achieved with the ACE method (Table S1). However, the main advantage of the CGE method compared to the ACE method is gene deletion or replacement in a single transformation step with selection for a double-crossover event. The ACE needs selection first, for a single crossover event and then another selection procedure for the double crossover event followed by recovery of the gene *pyrE* to allow cultivation under wildtype conditions which again requires its own selection procedure [15, 36]. Therefore, the CGE method can be applied on the wildtype strain, while a specific host strain with partial disruption of the gene *pyrE* is necessary for the ACE method [36].

Small plasmids (e.g., pMTL85141, 2963 bp [28]) can be removed by several re-plating steps of serial transfers onto non-selective medium, but this was found to be impossible for larger genome engineering plasmids (e.g., pDR, 8872 bp) [23]. Plasmid curing by utilization of CRISPR-Cas tools was shown in other microorganisms [32, 37, 38], but this principle was not designed for consecutive genome modifications in *C. pasteurianum* before. Nonetheless, a novel approach was verified in this study where each plasmid was designed to carry an additional DNA fragment of the next gene target to facilitate plasmid curing. Finally, strain DR-III with three genome modifications in the same mutant was successfully created by advanced genome editing procedures in this work. This achievement was previously not possible solely with the endogenous CRISPR-Cas method and therefore, the novelty of this work is that the CGE method addresses this drawback.

3.2 | Growth of the Wildtype R525 and Mutant DR-III on Mixed Substrates

C. pasteurianum is able to metabolize glycerol and glucose simultaneously [1] and this was used to study the influence of the genome modifications on the metabolism, which were designed to increase 1,3-PDO production and block the oxidative pathway from glycerol. Fermentations with 80 g L^{-1} glucose and 20 g L^{-1} glycerol were carried out with the mutant DR-II (Figure 3B,F) as well as the wildtype R525 as reference
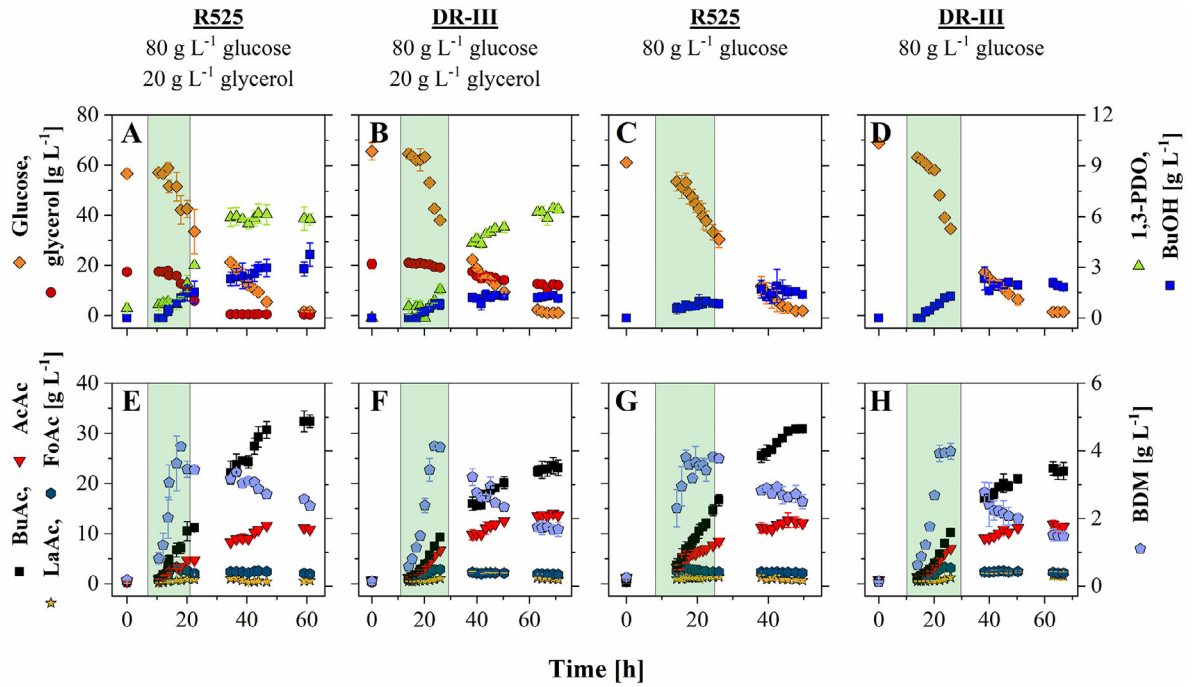
(Figure 3A,E) to determine if glycerol consumption was affected by the genome modifications. The fermentation with R525 started with a lag phase of around 10 h without macroscopic increase of biomass concentration, followed by the exponential growth phase with exponential increase in biomass concentration reaching a maximum growth rate of 0.26 ± 0.01 h^{-1} with R525. At 18 h, biomass concentration reached its highest value of 4.13 ± 0.06 g L^{-1} and started to decline. A specific glycerol consumption rate of 0.13 ± 0.01 g^{-1} g$_{biomass}$$^{-1}$ h^{-1} was observed and glycerol was completely consumed after a fermentation time of 34 h with R525. Glycerol depletion occurred before glucose was fully consumed after a fermentation time of 60 h with a specific glucose consumption rate of 0.41 ± 0.02 g^{-1} g$_{biomass}$$^{-1}$ h^{-1}.

The overall 1,3-PDO and butanol yields were calculated as 0.07 ± 0.01 and 0.05 ± 0.01 g g^{-1}, respectively, with R525 while acetate and butyrate yields reached values of 0.14 ± 0.00 and 0.45 ± 0.03 g g^{-1}, respectively. Calculated carbon distributions (Figure 4A) show a butanol distribution of 5.29 ± 0.95% and a 1,3-PDO distribution of 6.46 ± 0.66% with R525.

In contrast to R525, a 15% lower maximum growth rate of 0.22 ± 0.01 h^{-1} was reached with mutant DR-III in the exponential growth phase after a slightly longer lag phase of approximately 14 h and biomass concentration decreased after 26 h. Glucose was again fully consumed after 67 h and a 44% higher specific consumption rate of 0.59 ± 0.04 g^{-1} g$_{biomass}$$^{-1}$ h^{-1} with mutant DR-III was reached compared to R525. In contrast to glycerol depletion with R525, 12.07 ± 0.42 g L^{-1} glycerol was still remaining after 70 h with mutant DR-III. Moreover, a 39% lower specific glycerol consumption rate of 0.08 ± 0.00 g^{-1} g$_{biomass}$$^{-1}$ h^{-1} was observed with mutant DR-III compared to R525. Since glycerol consumption in mutant DR-III was lower, 1,3-PDO yield was calculated as 0.09 ± 0.01 g g^{-1} which is 29% higher compared to R525. The improvement in 1,3-PDO production can also be observed with a higher carbon distribution of 9.56 ± 0.61% with mutant DR-III compared to R525 (Figure 4A). Butanol, acetate and butyrate yields were calculated as 0.02 ± 0.00, 0.20 ± 0.02, and 0.35 ± 0.04 g g^{-1}, respectively. Therefore, butanol and butyrate yields are lower compared to R525 and higher for acetate. This is reflected in lower butanol carbon distributions of 2.63 ± 0.32% with mutant DR-III compared to the distribution with R525. As summarized in Figure 3, the results show that the genome modifications had a clear influence on glycerol utilization and an increase in 1,3-PDO yield was observed due to deletion of the oxidative pathway. However, when the molar 1,3-PDO yield was calculated for mutant DR-III with the assumption that glycerol was the only substrate for 1,3-PDO production, a value of 0.93 ± 0.19 mol mol^{-1} was obtained, indicating that a part of the glycerol is likely still converted into dihydroxyacetone (DHA). The reason might be the second gene encoding glycerol dehydrogenase (*dhaD2*) which would be a possible future deletion target to completely block conversion of glycerol to DHA.

3.3 | Growth of the Wildtype R525 and Mutant DR-III on Glucose

In order to compare the results with mutant DR-III, control fermentations with wildtype R525 were carried out with

R525	DR-III	R525	DR-III
80 g L^{-1} glucose	80 g L^{-1} glucose	80 g L^{-1} glucose	80 g L^{-1} glucose
20 g L^{-1} glycerol	20 g L^{-1} glycerol		

	R525 (80 g L^{-1} glucose, 20 g L^{-1} glycerol)	DR-III (80 g L^{-1} glucose, 20 g L^{-1} glycerol)	R525 (80 g L^{-1} glucose)	DR-III (80 g L^{-1} glucose)
μ_{max} [h^{-1}]	0.26 ± 0.01	0.22 ± 0.01	0.21 ± 0.06	0.23 ± 0.00
q_{glu} [g g^{-1} h^{-1}]	0.41 ± 0.02	0.59 ± 0.04	0.53 ± 0.04	0.75 ± 0.07
q_{gly} [g g^{-1} h^{-1}]	0.13 ± 0.01	0.08 ± 0.00	/	/
$Y_{1,3\text{-PDO}/(glu+gly)}$ [g g^{-1}]	0.07 ± 0.01	0.09 ± 0.01	/	/
$Y_{butanol/(glu+gly)}$ [g g^{-1}]	0.05 ± 0.01	0.02 ± 0.00	0.02 ± 0.00	0.03 ± 0.00
$Y_{acetate/(glu+gly)}$ [g g^{-1}]	0.14 ± 0.00	0.20 ± 0.02	0.18 ± 0.01	0.16 ± 0.01
$Y_{butyrate/(glu+gly)}$ [g g^{-1}]	0.45 ± 0.03	0.35 ± 0.04	0.52 ± 0.00	0.33 ± 0.03

Figure 3 | Batch fermentation data of R525 and mutant DR-III. Fermentations were carried out with addition of 100 mg L^{-1} FeSO$_4$*7H$_2$O under iron excess conditions, pH maintained at 6.5, temperature controlled at 35°C and stirrer set to 400 rpm. The error bars show the standard deviation from fermentations conducted in duplicates and the green colored background shows the exponential growth phase. AcAc indicates acetate; BDM, bio dry mass; BuAc, butyrate; BuOH, butanol; FoAc, formate; glu, glucose; gly, glycerol; LaAc, lactate.

supplementation of 80 g L^{-1} glucose as the sole carbon source (Figure 3C,G). The lag phase of estimated 8 h was followed by the exponential growth phase reaching a maximum growth rate of 0.21 ± 0.06 h^{-1} and highest biomass concentration was reached after 24 h with R525. The glucose was completely consumed after 48 h with an overall specific consumption rate of 0.53 ± 0.04 g^{-1} g$_{biomass}$ h^{-1}. The main products from glucose fermentations were formed after the lag phase and these are acetate and butyrate with yields of 0.18 ± 0.01 and 0.52 ± 0.00 g g^{-1}, respectively, while a butanol yield of 0.02 ± 0.00 g g^{-1} was determined. The carbon distributions from glucose fermentations (Figure 4B) show a butanol distribution of $2.54 \pm 0.26\%$ with R525.

Following a lag phase of roughly 10 h with mutant DR-III (Figure 3 D,H), a 10% higher maximum growth rate of 0.23 ± 0.00 h^{-1} was calculated for the exponential growth phase and highest biomass concentration was reached after 26 h with mutant DR-III. A 42% higher specific glucose consumption rate of 0.75 ± 0.07 g^{-1} g$_{biomass}$ $^{-1}$ h^{-1} was reached and all glucose was consumed after 63 h. Similar yields compared to R525 were calculated for butanol and acetate as 0.03 ± 0.00 and 0.16 ± 0.01 g g^{-1}, respectively, with mutant DR-III. Butyrate shows a notable 37% lower yield of 0.33 ± 0.03 g g^{-1} compared to R525. The carbon distributions (Figure 4B) show a slightly higher butanol distribution of $4.44 \pm 0.46\%$ with mutant DR-III compared to R525. 1,3-PDO productions of up to 0.97 ± 0.44 g L^{-1} for
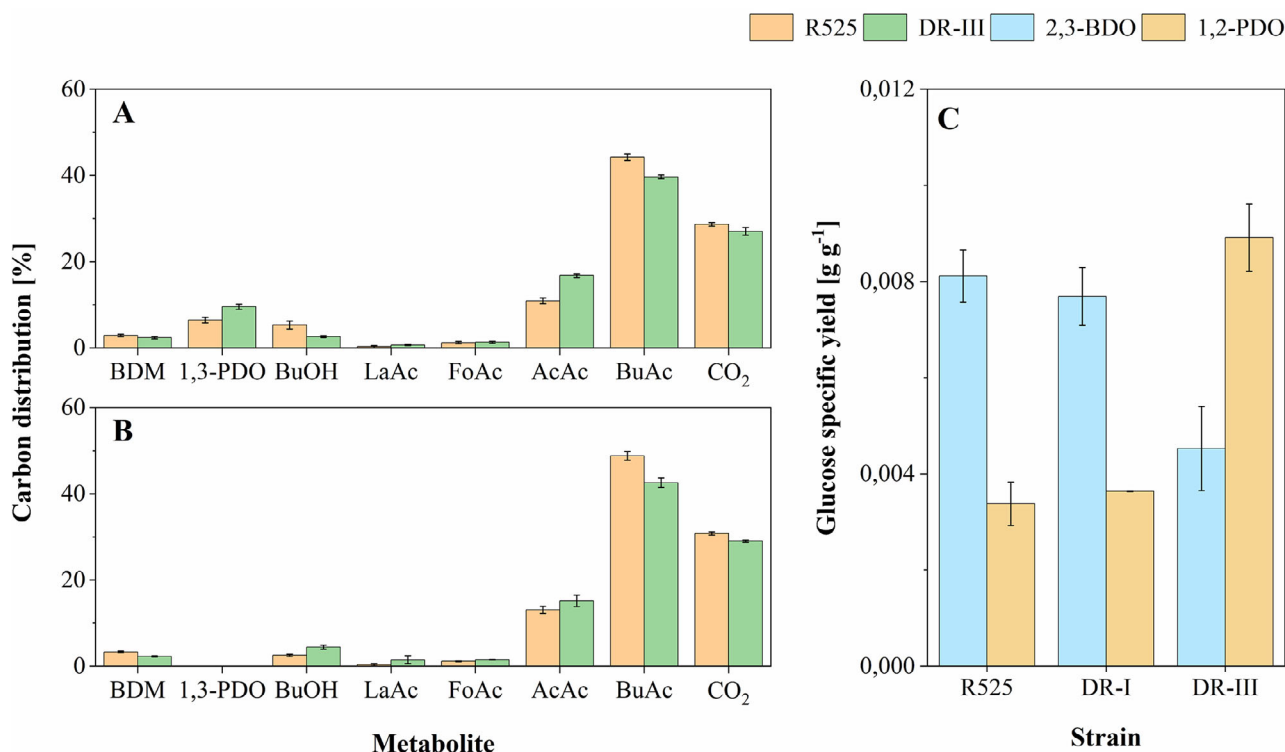
Figure 4 | Carbon distributions and 2,3-BDO and 1,2-PDO yield. (A) Carbon distributions from fermentations with 80 g L^{-1} glucose and 20 g L^{-1} glycerol. (B) Carbon distributions from fermentations with 80 g L^{-1} glucose. (C) Glucose specific yields of 2,3-BDO and 1,2-PDO for fermentations with R525, DR-I, and DR-III with 80 g L^{-1} glucose. AcAc indicates acetate; BuAc, butyrate; BuOH, butanol, BDM, bio dry mass; FoAc, formate; LaAc, lactate. The error bars show the standard deviation from fermentations conducted in duplicates.

the mutant DR-III were measured using HPLC in the glucose fermentations. However, 1,3-PDO concentrations of only below 10 mg L^{-1} were detected in the samples measured by GC-MS.

Therefore, expression of the genes *GPD1* and *GPP2* was apparently not enough to produce 1,3-PDO in sufficient amounts from glucose. A lack of reducing equivalents (NADH) in obligate anaerobic bacteria could be a possible reason. Only one NADH molecule is released in the conversion steps from the glycolysis intermediate glyceraldehyde-3-phosphate (GAP) to pyruvate. However, there are two NADH molecules needed for production of 1,3-PDO from dihydroxyacetone phosphate (DHAP) (Figure 1). Therefore, there is always an undersupply and production of 1,3-PDO from glucose is probably not favored by the cells. In contrast, facultative anaerobic bacteria were successfully engineered: Deletion, upregulation or overexpression of a total of 33 genes in *K. pneumoniae* enabled production of 62 g L^{-1} 1,3-PDO from glucose in fed-batch culture [9] and 110.4 g L^{-1} were reached by metabolic engineering of an efficient *C. glutamicum* strain [10]. However, the introduction of a large set of genes was necessary, because 1,3-PDO is not natively produced in these strains.

Another deletion target would include the gene encoding triosephosphate isomerase (*tpiA*) to split the metabolism so that half of the carbon can be used in pathways toward pyruvate and the other half can be directed to the desired 1,3-PDO. Further genetic modifications represent just one possible approach. Nonetheless, other analytical methods would also be necessary such as metabolic flux analysis, which can be combined with stable isotope tracers (e.g., ^{13}C) for more accurate results, to

quantify extracellular and intracellular carbon and electron fluxes [39]. The acquired information can be used to find potential bottlenecks and define appropriate metabolic engineering strategies to solve these. All fermentations were carried out under similar conditions, but bioprocess improvements, such as optimization of substrate concentration or pH value, can be made or other bioprocess modes such as fed-batch fermentation can be conducted to determine the impact on 1,3-PDO production.

3.4 | Detection of Unexpected Metabolites 1,2-Propanediol and 2,3-Butanediol

During analysis of data from glucose fermentations, a glucose specific yield of 3.38 ± 0.45 mg g^{-1} for 1,2-PDO was calculated for R525, but a yield of 8.11 ± 0.54 mg g^{-1} of another unexpected product 2,3-butanediol (2,3-BDO) was also determined (Figure 4C). For mutant DR-III, yields of 8.91 ± 0.70 and 4.53 ± 0.88 mg g^{-1} for 1,2-PDO and 2,3-BDO, respectively, were determined. For comparison, measurements from glucose fermentations with mutant DR-I were also evaluated. No butanol dehydrogenase genes were deleted in mutant DR-I, which was initially created to examine the effect of these deletions on 1,3-PDO production from glucose, but 1,3-PDO concentrations of only below 10 mg L^{-1} were measured. However, glucose specific yields of 3.64 ± 0.01 and 7.69 ± 0.60 mg g^{-1} for 1,2-PDO and 2,3-BDO, respectively, were reached with mutant DR-I which result in 59% lower 1,2-PDO and 70% higher 2,3-BDO yields compared to mutant DR-III.
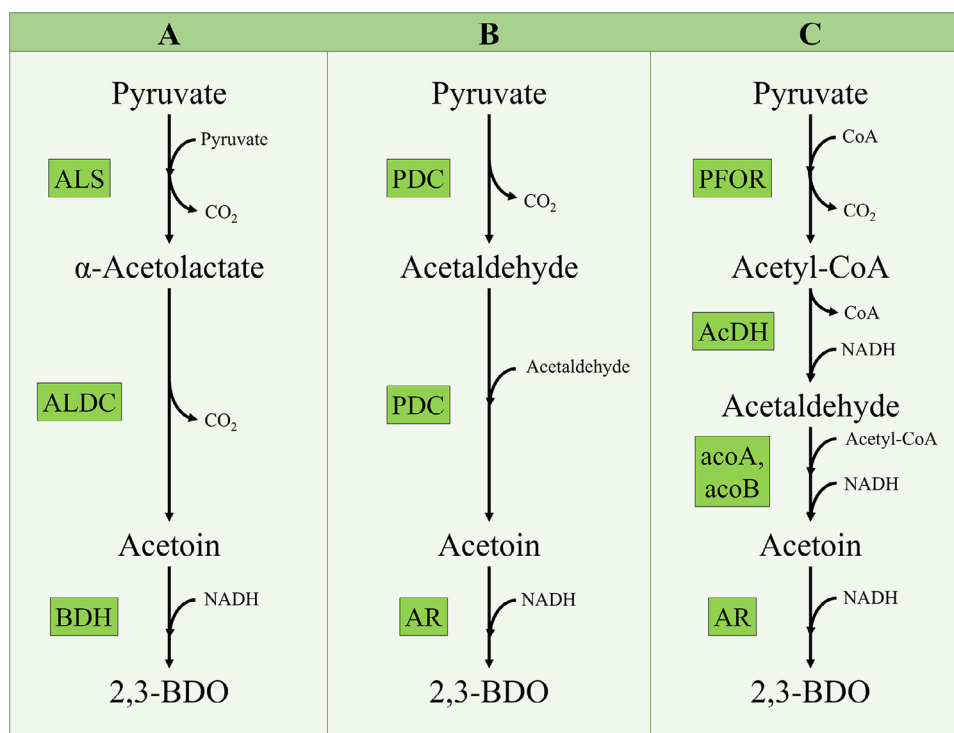
Figure 5 | Possible pathways for the production of 2,3-BDO from pyruvate. (A) Production via α-acetolactate, (B) production via condensation of two acetaldehyde molecules, (C) production via condensation of acetaldehyde and acetyl-CoA. AcDH indicates acetaldehyde dehydrogenase; acoA and acoB, acetoin oxidoreductase subunits alpha and beta; ALDC, α-acetolactate decarboxylase; ALS, α-acetolactate synthase; AR, acetoin reductase; BDH, 2,3-BDO dehydrogenase; PDC, pyruvate decarboxylase; PFOR: pyruvate:ferredoxin oxidoreductase.

The deletion of two genes encoding butanol dehydrogenases most likely had no effect on 1,3-PDO production from glucose fermentations, but instead the carbons were directed to higher 1,2-PDO and lower 2,3-BDO production. It was previously reported that *C. pasteurianum* is also able to produce 1,2-PDO under certain conditions. 1,2-PDO can be formed via methylglyoxal which is formed from DHAP by the methylglyoxal synthase *mgsA* [12] and this gene can be a deletion target to block production of undesired 1,2-PDO. On the one hand, the finding of a new phenotype shows that formation of 2,3-BDO was not directly triggered by the introduced genome modifications, but on the other hand, it was not reported to be produced by *C. pasteurianum* before. Although this phenotype with production of 2,3-BDO was already reported for *C. pasteurianum* NRRL B-598 [40], this strain was later re-classified to *C. beijerinckii* NRRL B-598 [41] showing that this strain is different to the one used in this study.

Other *Klebsiella* [42] or *Saccharomyces* [43] strains can produce 2,3-BDO and in one of possible pathways (Figure 5A), pyruvate is decarboxylated by the enzyme α-acetolactate synthase (ALS) to form α-acetolactate. Next, further conversion in another decarboxylation reaction into acetoin by α-acetolactate decarboxylase (ALDC) occurs. Finally, the acetoin intermediate undergoes a reduction reaction to produce 2,3-BDO with help of butanediol dehydrogenase (BDH) or acetoin reductase (AR) [43]. The genome of *S. cerevisiae* however shows a second possible pathway (Figure 5B) from acetaldehyde and in this case the pyruvate decarboxylase (PDC) catalyzes the condensation reaction between two acetaldehyde molecules [43, 44]. In the third possible pathway (Figure 5C), acetoin is produced by condensation of acetaldehyde

and acetyl-CoA by an acetoin dehydrogenase E1 complex (acoA, acoB).

Overexpression of the genes *acoA* and *acoB* from *Bacillus subtilis* in *S. cerevisiae* increased the 2,3-BDO production [43], so based on screening of the *C. pasteurianum* genome (Supporting Information 6), it is likely that 2,3-BDO is produced from acetyl-CoA and acetaldehyde, resulting in the observed phenotype. In future studies, it would be possible to delete both genes *acoA* and *acoB* in a single mutant with the newly developed CGE method in order to verify that these genes are involved in the production of 2,3-BDO in *C. pasteurianum*.

4 | Concluding Remarks

A consecutive genome engineering method (CGE) was successfully developed and it allows the performance of several consecutive editing steps in contrast to preceding studies where mainly one modification was considered at a time. It is the first time that the endogenous CRISPR-Cas method was applied to delete multiple genes in *C. pasteurianum* with the CGE method and it made consecutive genome modification procedures more compact and simpler in comparison to the more complex ACE method. This opens a broad range of novel possibilities for researchers to alter the genome of *C. pasteurianum* for desired applications such as deletion of competing pathways. This would also further improve the understanding of the metabolism of *C. pasteurianum*. The regulation of reducing power in *C. pasteurianum* R525 seems to be very sensitive and is a possible

burden for manipulating this strain to produce 1,3-PDO from glucose. The detected 2,3-BDO in this work was not reported to be produced by *C. pasteurianum* R525 before and it can be assumed that the 2,3-BDO pathway plays a role in consumption of excess NADH [45]. Overall, the most important changes necessary for *C. pasteurianum* R525 include modifications which reduce the flux to competing pathways in order to create a promising *C. pasteurianum* R525 host strain for 1,3-PDO production from glucose.

References

1. W. Sabra, W. Wang, S. Surandram, et al., "Fermentation of Mixed Substrates by *Clostridium Pasteurianum* and Its Physiological, Metabolic and Proteomic Characterizations," *Microbial Cell Factories* 15 (2016): 114.

2. H. Biebl, "Fermentation of Glycerol by *Clostridium Pasteurianum*-Batch and Continuous Culture Studies," *Journal of Industrial Microbiology & Biotechnology* 27 (2001): 18–26.

3. R. Schmitz, W. Sabra, P. Arbter, et al., "Improved Electrocompetence and Metabolic Engineering of *Clostridium Pasteurianum* Reveals a New Regulation Pattern of Glycerol Fermentation," *Engineering in Life Sciences* 19 (2019): 412–422.

4. T. Kaeding, J. DaLuz, J. Kube, and A.-P. Zeng, "Integrated Study of Fermentation and Downstream Processing in a Miniplant Significantly Improved the Microbial 1,3-Propanediol Production From Raw Glycerol," *Bioprocess and Biosystems Engineering* 38 (2015): 575–586.

5. C. Zhang, P. Traitrongsat, and A.-P. Zeng, "Electrochemically Mediated Bioconversion and Integrated Purification Greatly Enhanced Co-Production of 1,3-Propanediol and Organic Acids From Glycerol in an Industrial Bioprocess," *Bioprocess and Biosystems Engineering* 46, no. 4 (2023): 565–575.

6. C. Zhang, S. Sharma, C. Ma, and A.-P. Zeng, "Strain Evolution and Novel Downstream Processing With Integrated Catalysis Enable Highly Efficient Coproduction of 1,3-Propanediol and Organic Acid Esters From Crude Glycerol," *Biotechnology and Bioengineering* 119 (2022): 1450–1466.

7. M. Emptage, S. L. Haynie, L. A. Laffend, et al., "Process for the Biological Production of 1,3-Propanediol With High Titer" (US Patent No. 6,514,733 B1, 2003).

8. C. E. Nakamura, A. A. Gatenby, A. K.-H. Hsu, et al., "Method for the production of 1, 3-propanediol by recombinant microorganisms" (US Patent No. 6,013,494, 2000).

9. S. Lama, E. Seol, and S. Park, "Development of *Klebsiella pneumoniae* J2B as Microbial Cell Factory for the Production of 1,3-Propanediol From Glucose," *Metabolic Engineering* 62 (2020): 116–125.

10. Z. Li, Y. Dong, Y. Liu, et al., "Systems Metabolic Engineering of *Corynebacterium Glutamicum* for High-Level Production of 1,3-Propanediol From Glucose and Xylose," *Metabolic Engineering* 70 (2022): 79–88.

11. Y. Hong, P. Arbter, W. Wang, et al., "Introduction of Glycine Synthase Enables Uptake of Exogenous Formate and Strongly Impacts the Metabolism in *Clostridium Pasteurianum*," *Biotechnology and Bioengineering* 118 (2020): 1366–1380.

12. M. E. Pyne, S. Sokolenko, X. Liu, et al., "Disruption of the Reductive 1,3-Propanediol Pathway Triggers Production of 1,2-Propanediol for Sustained Glycerol Fermentation by *Clostridium Pasteurianum*," *Applied and Environmental Microbiology* 82 (2016): 5375–5388.

13. M. E. Pyne, M. R. Bruder, M. Moo-Young, et al., "Harnessing Heterologous and Endogenous CRISPR-Cas Machineries for Efficient Markerless Genome Editing in *Clostridium*," *Scientific Reports* 6 (2016): 25666.

14. D. Ortega, "*Synthetic Biology & Metabolic Engineering of* Clostridium pasteurianum" (Doctoral diss., University of Nottingham, 2020).

15. K. M. Schwarz, A. Grosse-Honebrink, K. Derecka, et al., "Towards Improved Butanol Production Through Targeted Genetic Modification of *Clostridium Pasteurianum*," *Metabolic Engineering* 40 (2017): 124–137.

16. B. Zetsche, M. Heidenreich, P. Mohanraju, et al., "Multiplex Gene Editing by CRISPR-Cpf1 Using a Single crRNA Array," *Nature Biotechnology* 35 (2017): 31–34.

17. R. E. Cobb, Y. Wang, and H. Zhao, "High-Efficiency Multiplex Genome Editing of Streptomyces Species Using an Engineered CRISPR/Cas System," *ACS Synthetic Biology* 4 (2015): 723–728.

18. L. Li, K. Wei, G. Zheng, et al., "CRISPR-Cpf1-Assisted Multiplex Genome Editing and Transcriptional Repression in *Streptomyces*," *Applied and Environmental Microbiology* 84 (2018): e00827–18.

19. Y. Jiang, B. Chen, C. Duan, et al., "Multigene Editing in the *Escherichia coli* Genome via the CRISPR-Cas9 System," *Applied and Environmental Microbiology* 81 (2015): 2506–2514.

20. W. Jiang, D. Bikard, D. Cox, et al., "RNA-Guided Editing of Bacterial Genomes Using CRISPR-Cas Systems," *Nature Biotechnology* 31 (2013): 233–239.

21. M. Diallo, R. Hocq, F. Collas, et al., "Adaptation and Application of a Two-Plasmid Inducible CRISPR-Cas9 System in *Clostridium beijerinckii*," *Methods (San Diego, Calif.)* 172 (2020): 51–60.

22. F. Wasels, J. Jean-Marie, F. Collas, et al., "A Two-Plasmid Inducible CRISPR/Cas9 Genome Editing Tool for *Clostridium Acetobutylicum*," *Journal of Microbiological Methods* 140 (2017): 5–11.

23. Y. Hong, "*Engineering of Clostridium pasteurianum for Formate Uptake and Application of Unsupervised Learning From Fermentation Analysis*" (Doctoral dissertation, Hamburg University of Technology, published by Dr. Hut, München, Germany, 2022). http://hdl.handle.net/11420/12694.

24. J. Albertyn, S. Hohmann, J. M. Thevelein, and B. A. Prior, "*GPD1*, Which Encodes Glycerol-3-Phosphate Dehydrogenase, Is Essential for Growth Under Osmotic Stress in *Saccharomyces Cerevisiae*, and Its Expression Is Regulated by the High-Osmolarity Glycerol Response Pathway," *Molecular and Cellular Biology* 14 (1994): 4135–4144.

25. P. Eriksson, L. André, R. Ansell, et al., "Cloning and Characterization of *GPD2*, a Second Gene Encoding sn-Glycerol 3-Phosphate Dehydrogenase (NAD+) in *Saccharomyces Cerevisiae*, and Its Comparison With *GPD1*," *Molecular Microbiology* 17 (1995): 95–107.

26. A. Poehlein, A. Grosse-Honebrink, Y. Zhang, et al., "Complete Genome Sequence of the Nitrogen-Fixing and Solvent-Producing *Clostridium Pasteurianum* DSM 525," *Genome Announcements* 3 (2015): e01591-14.

27. M. E. Pyne, M. Moo-Young, D. A. Chung, and C. P. Chou, "Development of an Electrotransformation Protocol for Genetic Manipulation of *Clostridium Pasteurianum*," *Biotechnology for Biofuels* 6 (2013): 50.

28. J. T. Heap, O. J. Pennington, S. T. Cartman, and N. P. Minton, "A Modular System for *Clostridium* Shuttle Plasmids," *Journal of Microbiological Methods* 78 (2009): 79–85.

29. R. Schmitz, "*Metabolic Engineering von Clostridium Pasteurianum zur Optimierung der Biobutanolproduktion*" (Doctoral dissertation, Hamburg University of Technology, Hamburg, 2018).

30. C. Groeger, W. Wang, W. Sabra, et al., "Metabolic and Proteomic Analyses of Product Selectivity and Redox Regulation in *Clostridium Pasteurianum* Grown on Glycerol Under Varied Iron Availability," *Microbial Cell Factories* 16 (2017): 64.

31. J. T. Heap, S. A. Kuehne, M. Ehsaan, et al., "The ClosTron: Mutagenesis in *Clostridium* Refined and Streamlined," *Journal of Microbiological Methods* 80 (2010): 49–55.

32. E. R. Westra, P. B. G. van Erp, T. Künne, et al., "CRISPR Immunity Relies on the Consecutive Binding and Degradation of Negatively Supercoiled Invader DNA by Cascade and Cas3," *Molecular Cell* 46 (2012): 595–605.

33. M. L. Hochstrasser and J. A. Doudna, "Cutting It Close: CRISPR-Associated Endoribonuclease Structure and Function," *Trends in Biochemical Sciences* 40 (2015): 58–66.

34. H. Biebl and N. Pfennig, "Isolation of Members of the family *Rhodospirillaceae*," in *The Prokaryotes: A Handbook on Habitats, Isolation, and Identification of Bacteria* (Springer, Berlin, Germany, 1981), 267–273, https://doi.org/10.1007/978-3-662-13187-9_14.

35. T. Utesch, W. Sabra, C. Prescher, et al., "Enhanced Electron Transfer of Different Mediators for Strictly Opposite Shifting of Metabolism in *Clostridium Pasteurianum* Grown on Glycerol in a New Electrochemical Bioreactor," *Biotechnology and Bioengineering* 116 (2019): 1627–1643.

36. A. Grosse-Honebrink, "*Forward and Reverse Genetics in Industrially Important Clostridia*" (Doctoral diss., University of Nottingham, 2017).

37. D. Bikard, C. W. Euler, W. Jiang, et al., "Exploiting CRISPR-Cas Nucleases to Produce Sequence-Specific Antimicrobials," *Nature Biotechnology* 32 (2014): 1146–1150.

38. B. J. Caliando and C. A. Voigt, "Targeted DNA Degradation Using a CRISPR Device Stably Carried in the Host Genome," *Nature Communications* 6 (2015): 6989.

39. M. R. Antoniewicz, "A Guide to Metabolic Flux Analysis in Metabolic Engineering: Methods, Tools and Applications," *Metabolic Engineering* 63 (2021): 2–12.

40. M. Gungormusler, C. Gonen, G. Ozdemir, and N. Azbar, "1,3-Propanediol Production Potential of *Clostridium Saccharobutylicum* NRRL B-643," *New Biotechnology* 27 (2010): 782–788.

41. K. Sedlar, J. Kolek, I. Provaznik, and P. Patakova, "Reclassification of Non-Type Strain *Clostridium Pasteurianum* NRRL B-598 as *Clostridium Beijerinckii* NRRL B-598," *Journal of Biotechnology* 244 (2017): 1–3.

42. M. Metsoviti, K. Paraskevaidi, A. Koutinas, et al., "Production of 1,3-Propanediol, 2,3-Butanediol and Ethanol by a Newly Isolated *Klebsiella oxytoca* Strain Growing on Biodiesel-Derived Glycerol Based media," *Process Biochemistry* 47 (2012): 1872–1882.

43. S.-J. Kim, J.-W. Kim, Y.-G. Lee, et al., "Metabolic Engineering of *Saccharomyces Cerevisiae* for 2,3-Butanediol Production," *Applied Microbiology and Biotechnology* 101 (2017): 2241–2250.

44. E. González, M. R. Fernández, C. Larroy, et al., "Characterization of a (2R,3R)-2,3-Butanediol Dehydrogenase as the *Saccharomyces Cerevisiae* YAL060W Gene Product. Disruption and Induction of the Gene," *Journal of Biological Chemistry* 275 (2000): 35876–35885.

45. S. Maina, A. A. Prabhu, N. Vivek, et al., "Prospects on Bio-Based 2,3-Butanediol and Acetoin Production: Recent Progress and Advances," *Biotechnology Advances* 54 (2022): 107783.

Supporting Information

Additional supporting information can be found online in the Supporting Information section.